PHYSICAL REVIEW A VOLUME 57, NUMBER 1 JANUARY 1998

# Phase change of a probe due to oscillation of cold atoms in an optical standing wave

M. Kozuma,[1,*] K. Nakagawa,[2,†] W. Jhe,[3,‡] and M. Ohtsu[1,4,*,§]
[1]*Interdisciplinary Graduate School of Science and Engineering, Tokyo Institute of Technology, 4259, Nagatsuta-cho, Midori-ku, Yokohama 226, Japan*
[2]*Tokyo Institute of Polytechnics, 1583, Iiyama-cho, Atugi 243-02, Japan*
[3]*Department of Physics, Seoul National University, Seoul 151-742, Korea*
[4]*Kanagawa Academy of Science and Technology, KSP East 408, 3-2-1 Sakado, Takatsu-ku, Kawasaki 213, Japan*
(Received 5 March 1997)

We abruptly subject laser-cooled $^{87}$Rb atoms to the one-dimensional, blue-detuned, optical standing-wave potential generated by two crossed probe laser beams and detect the phase change of the probe beam due to cold-atom dynamics. Damped oscillations of the observed phase signal are attributed to a temporal change of the root-mean-square position of the cold atoms relative to the minima of the periodic optical potential. The damping rate is in good agreement with numerical results, which take into account the potential anharmonicity but neglect spontaneous emission. The agreement indicates that the decay is mainly caused by dephasing due to trap anharmonicity. For sufficient low initial temperature, our calculations show quantum revivals of the wave-packet oscillation. [S1050-2947(98)51001-3]

PACS number(s): 32.80.Pj

Laser-cooling techniques make it possible to prepare very cold atomic samples whose center-of-mass motion can be controlled by optical potentials. When such cold atoms are confined by a periodic optical potential, atomic energies are quantized and discrete band structures appear. The discrete vibrational energy spectrum has been observed using stimulated Raman transitions [1,2] and resonance fluorescence [3]. More recently, we have observed the oscillation of the atomic position in the time domain (i.e., pendulum motion of the center of the atomic density distribution) via the transient response [4,5] of recoil-induced resonance [6].

From a quantum-mechanical point of view, such an oscillation is the result of coherence between the $n$th and $(n+1)$th vibrational states. The damping rate of the transient signal is related to the spectral widths of the sidebands for absorption and emission [1–3], since the sidebands are associated with the autocorrelation of the atomic oscillation. It was recently realized that the observed signal decay rate was much smaller than the inelastic optical scattering rate predicted by Lamb-Dicke theory [7]. Consequently, it was suggested that for a perfectly harmonic potential, the signal damping rate be determined by the cooling rate, which is much smaller than the inelastic scattering rate.

In our previous work [4,5] the oscillation of the mean atomic position was observed by the change in intensity of the probe beam. Alternatively, one can detect the change of phase of the probe beam. In this case, in contrast to intensity detection, one observes the temporal change of the root-mean-square (rms) position spread of cold atoms in the potential wells. Thus, the phase of the probe light allows one to measure periodic contraction and expansion of the atomic density distribution caused by coherence between the $n$th and $(n+2)$th vibrational states. By detecting both intensity and phase signals, one can obtain complementary information on the atomic dynamics in the potential. It also opens up the possibility of active control of atomic motion by temporal change of the optical potential.

In this paper, we describe an observation of the phase change of the transmitted probe beam caused by the oscillation of the rms position of trapped atoms. The rms position of cold atoms has also been measured in optical lattice experiments using Bragg scattering [8–11] and fluorescence [12]. The method presented here has the advantage that the atomic dynamics is not perturbed by an additional probe laser beam.

In our experiment, a cold cloud of $^{87}$Rb atoms is prepared by a magneto-optical trap (MOT) [13] and polarization gradient cooling (PGC) [14] in a vapor cell. The $5S_{1/2}F=2 \rightarrow 5P_{3/2}F=3$ cyclic transition of the $^{87}$Rb $D_2$ line was used for cooling. Figure 1 shows our experimental setup to observe recoil-induced resonance and its transient response. Inside the cold sample, two probe beams [with wave vectors $\vec{k}_1$, $\vec{k}_2$ ($\vec{q} \equiv \vec{k}_2 - \vec{k}_1$), angular frequencies $\omega_1, \omega_2$ ($\delta \equiv \omega_2 - \omega_1$) detuned from the cooling transition by $\Delta$ ($\Delta \gg \delta$), and parallel linear polarizations] are crossed at an angle $\theta$. These two probe beams are generated from the same extended cavity diode laser, each one having passed through a 20-$\mu$m pinhole to obtain a uniform wave front. Under these conditions, an optical potential proportional to $\cos(qr_q - \delta t)$ is generated in the beam-crossing area. The velocity of the optical potential in the laboratory frame, $v_0 = \delta/q$ along $\vec{q}$ ($q \equiv |\vec{q}|$), is controlled by changing $\delta$. Here, $r_q$ is the projection of the position vector on $\vec{q}$, and the spatial period of the potential is $2\pi/q$. One of the transmitted probes is divided by a beam splitter (BS), one part being detected by a photodetector PD1 for intensity measurement, and the other one being mixed by a 1-mm-thick étalon plate (ET) and then detected by PD2 for phase measurement. Reflectivities of the front and rear faces of the ET are 38% and 100%, respec-

*FAX: +81-45-921-1204.
†FAX: +81-462-42-9511.
‡FAX: +82-2-884-3002.
§FAX: +81-44-819-2072.

 

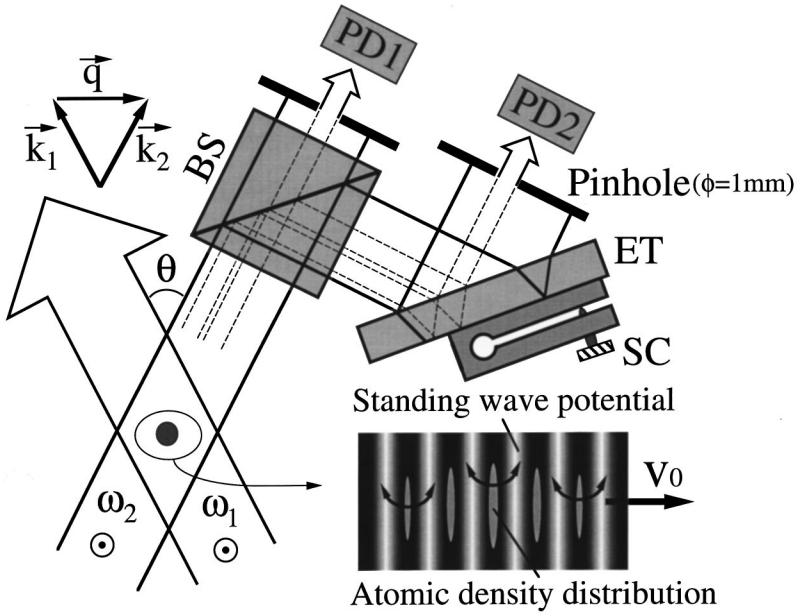


FIG. 1. Experimental scheme to observe recoil-induced resonance and its transient response.

tively. Because the diameter of the probe beams (5 mm) is bigger than the size of the atomic cloud ($<1$ mm), only the central part of the probe interacts with the cold atoms. The central and the outer part of the probe beam are overlapped by the ET, and thus the output signal of PD2 is a convolution of both the intensity and phase changes of the transmitted probe beam. The reflection angle of the ET is adjusted by a fine screw (SC) in such a way that phase sensitivity is maximized.

First the temperature of the cold atoms is measured by using recoil-induced resonance [4,6]. We record the output of PD1 versus the frequency difference $\delta$, and estimate the temperature to be as low as 4.7 $\mu$K. Here, the intensity of the probe beams is 4.2 mW/cm$^2$, $\theta=12.5°$, the frequency difference $\delta$ is scanned at a rate $d(\delta/2\pi)/dt=54$ kHz/ms, and $\Delta/2\pi=+920$ MHz. The large detuning ensures that the optical potential is shallow enough that the atomic momentum distribution is not perturbed.

Next, we observe the change in both the intensity and phase of the transmitted probe due to the transient response of recoil-induced resonance. Temporal changes of PD1 and PD2 outputs are monitored for fixed $\delta$, i.e., the cold atoms are exposed to one-dimensional standing waves with a constant, $\delta$-dependent drift speed. Figure 2 shows typical photodetector signals for three frequency differences and for the intensity and crossing angle stated above. The detuning is $\Delta/2\pi=+90$ MHz, and the frequency difference $\delta/2\pi$ is set smaller than 6 kHz. Under these conditions, the atomic kinetic energy in the frame of the moving optical potential, $(m\delta/q)^2/2m \leqslant (3.7\hbar k)^2/2m$, is much smaller than the optical potential depth $(8.9\hbar k)^2/2m$, and thus localized atomic motion is achieved. Atoms preferably populate the $F=2, m=0$ ground state due to optical pumping. Therefore, our optical potential depth refers to the transition $F=2, m=0 \rightarrow F'=3, m=0$.

When $\delta/2\pi=6$ kHz [Fig. 2(a)], damped oscillation of the output from PD1 is observed, which reflects the oscillation of the mean atomic position relative to the slowly moving optical potential [5]. Such an oscillation of the mean atomic position cannot be induced when atoms are exposed to a stationary standing wave because of the symmetry of the system. We actually observed that the damped oscillation of PD1 output vanished at $\delta/2\pi=-0.4$ kHz [Fig. 2(b)]. We interpret this as follows: Due to an intensity imbalance between the MOT and PGC counterpropagating cooling laser beams, the atoms were cooled to a nonzero average velocity. Therefore, a small $\delta$ (i.e., small drifting speed of the potential) was needed to compensate that motion. Even though the oscillation of the output of PD1 vanished, we still observed a damped oscillation of the PD2 signal [Fig. 2(c)]. This implies that the residual atomic dynamics caused an oscillatory phase change of the probe beam but no intensity modulation. The oscillation frequencies of Figs. 2(a) and 2(c) are 5.38 $\pm$0.05 kHz and 9.0$\pm$0.1 kHz, respectively.

We now present the physical mechanism responsible for

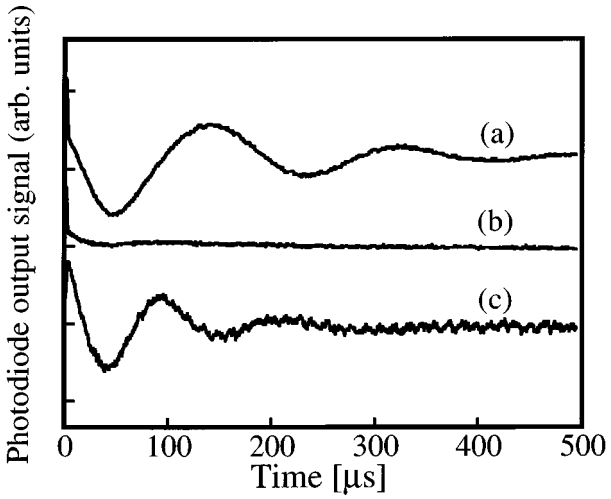


FIG. 2. The output signals of two photodetectors [(a), (b)] PD1 and (c) PD2. The frequency differences for each signal were (a) $\delta/2\pi=6$ kHz and [(b), (c)] $\delta/2\pi=-0.4$ kHz, respectively.

the observed oscillatory phase change. The intensity and phase change of the probe arise from a recoil-induced resonance and can be represented by the imaginary and real part of the induced polarization $P$, respectively, approximately given by

$$P \cong -\frac{2\mu\Omega}{\Delta} \int dr_q \exp[i(qr_q - \delta t)]\overline{\psi^*(r_q,t)\psi(r_q,t)}. \tag{1}$$

Here $\Omega$ and $\mu$ are the Rabi frequency and the transition dipole moment, respectively. $\psi(r_q,t)$ is the atomic center-of-mass wave function, and $\overline{\psi^*(r_q,t)\psi(r_q,t)}$ represents the ensemble average of the density distribution for all of the atoms (atomic density grating), since they all contribute to the signal. From Eq. (1), we can understand that an intensity change of the transmitted probe beam originates in a modulation of the atomic density distribution proportional to $\sin(qr_q - \delta t)$. Because the optical potential has a periodicity of $\cos(qr_q - \delta t)$, the time evolution of the average atomic position relative to the minima of the periodic potential leads to the intensity change of the transmitted probe beam. On the other hand, a change of the rms position spread of the atoms relative to the potential minima affects only the real part of the polarization, implying that a temporal change of the rms position spread of the atoms manifests itself as a phase change of the probe beam. In Fig. 2, even when the intensity change vanished [Fig. 2(b)], a phase change was still observed [Fig. 2(c)]. Thus the damped oscillation of the observed phase change corresponds to an oscillation of the width of the position distribution.

In order to investigate the characteristics of signal decay, we simulated the atomic dynamics when cold atoms are nonadiabatically exposed to the stationary standing wave. We neglected spontaneous emission and calculated the time evolution of the atomic density operator, assuming that its initial value was given by a Maxwell-Boltzmann distribution with temperature $T$. The time evolution of the density operator after switching on the probe light abruptly was determined by the Hamiltonian, which consists of the atomic kinetic energy and the optical potential,

$$i\hbar\dot{\rho}_{p'p''} = \frac{1}{2m}(p'^2 - p''^2)\rho_{p'p''} - \frac{U_0}{4}(\rho_{p'-\hbar q p''} + \rho_{p'+\hbar q p''} - \rho_{p'p''+\hbar q} - \rho_{p'p''-\hbar q}), \tag{2}$$

where the density operator is given in momentum representation, and $U_0$ is the potential depth.

In Fig. 3, solid lines show the time evolution of the rms position spread of the atoms calculated by Eq. (2). Dashed lines are results calculated with Newton's equation in the same periodic potential. The crossing angle, detuning, and intensity of each probe beam were the same as in Fig. 2. The initial rms momentum $\Delta p_q$ of the atoms along $\vec{q}$ was set to (a) $\Delta p_q/\hbar q = 0$, (b) $\Delta p_q/\hbar q = 1$, and (c) $\Delta p_q/\hbar q = 17$, respectively. Here, Fig. 3(c) corresponds to our experimental condition of $T = 4.7\ \mu$K. In Fig. 3, the time is given in units of $2\pi/\omega$, where $\omega$ is the Bohr frequency between the lowest and first excited vibrational levels. Both the classical and quantum-mechanical results show that the oscillation of the rms position of the atoms damps rapidly due to the dephasing effect caused by the trap anharmonicity. When $\Delta p_q/\hbar q = 0$, a remarkable difference between classical and quantum simulations appears, which is a quantum revival of the atomic oscillation [solid curve in Fig. 3(a)]. [Our calculation shows that our optical potential contains approximately 50 discrete bound states. Under conditions such as in Fig. 3(a), the sudden turn-on of the potential excites the atoms to a distribution of vibrational levels whose mean excitation quantum number is 23. Here, the effect of the periodicity of the lattice and tunneling from one well to another is taken into account.] For large initial rms momentum of the atoms, such as in Fig. 3(b), and in particular in Fig. 3(c), the quantum revival, visible in Fig. 3(a), diminishes [solid curves in Figs. 3(b) and 3(c)]. Nevertheless, although the quantum calculation approaches the classical one for the calculation of Fig. 3(c), the calculation shows that a slight revival still exists [see inset of Fig. 3(c)].

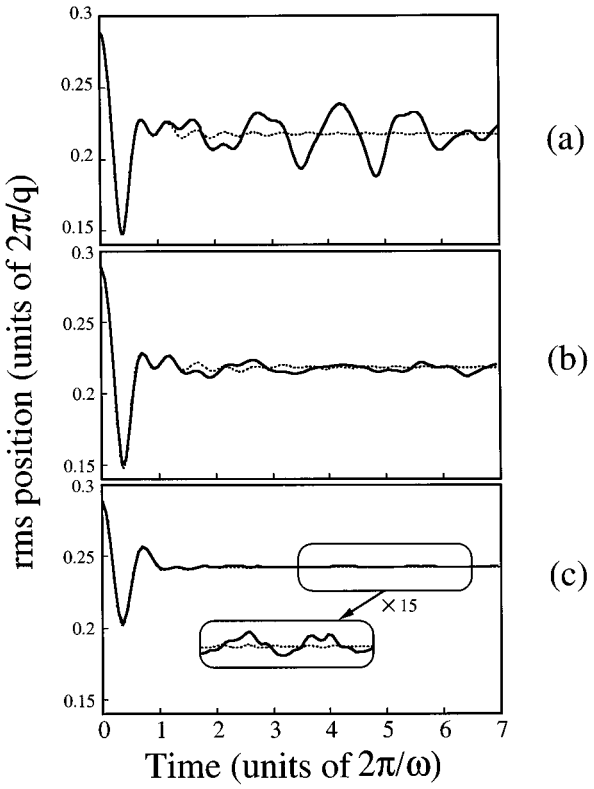


FIG. 3. Numerical results for the time evolution of the root-mean-square (rms) position of the atomic density distribution relative to the minima of the standing-wave potential. Solid and dotted lines are quantum and classical results, respectively. The rms position spreads were estimated inside one spatial period of the potential, $2\pi/q$. The initial rms momentum $\Delta p_q$ of the cold atoms along $\vec{q}$ are (a) $\Delta p_q/\hbar q = 0$, (b) $\Delta p_q/\hbar q = 1$, and (c) $\Delta p_q/\hbar q = 17$, respectively.

Figure 4 shows both (a) experimental [same as Fig. 2(c)] and (b) numerical results of the phase change signal of the transmitted probe, where Fig. 4(b) was calculated using Eqs. (1) and (2) for the conditions of Fig. 3(c). Figure 4(a) is in good agreement with Fig. 4(b), which indicates that the decay rate of the phase signal was mainly determined by dephasing due to trap anharmonicity. While a slight quantum

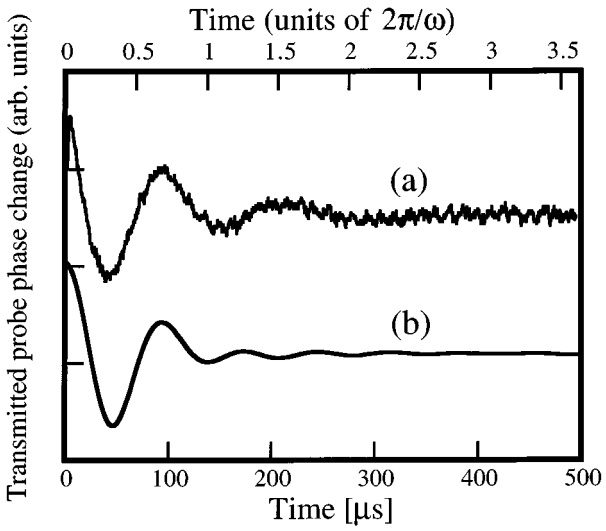


FIG. 4. (a) Experimental and (b) numerical results for the phase change signal of the transmitted probe. Note that (a) is identical to Fig. 2(c).

revival appears in Fig. 3(c), we did not observe such a revival in our experiment. We believe that there are two reasons why we could not observe the revival. First, our signal-to-noise ratio was insufficient. Second, the population of sublevels other than the $F=2$, $m=0$ state was not zero. Atoms in these sublevels experience optical potential depths shallower than that for the $F=2$, $m=0$ state due to the smaller relative transition strength, which causes an additional spread of frequencies and increases the damping rate of the atomic density grating oscillation. However, using a large crossing angle and a subrecoil cooling technique [15,16], the value of $\Delta p_q/\hbar q$ could be decreased such that the quantum revival of the atomic oscillation could be observed.

The calculated oscillation frequencies of the rms width (measured by PD2) and mean position (measured by PD1) are $(1.49\pm0.08)\omega$ and $(0.88\pm0.02)\omega$, which are smaller than $2\omega$ and $\omega$ due to the potential anharmonicity. The corresponding experimentally observed frequencies of $1.2\omega$ (9.0 kHz) and $0.73\omega$ (5.4 kHz) are 17% smaller than the numerical values. We believe this is because atoms in sublevels other than the $F=2$, $m=0$ state experience a shallower potential depth. The experimental value of the ratio of these frequencies is 1.7, which agrees perfectly with our theoretical result.

The authors wish to thank Dr. W. D. Phillips (NIST), Dr. G. Raithel (NIST), Dr. J. Lawall (NIST), Dr. C. I. Westbrook (CNRS), and Dr. A. Zvyagin (TIT) for their valuable comments and discussions. A part of this work was supported by the Japanese Society for the Promotion of Science for Young Scientists. W. Jhe is grateful to the Ministry of Science and Technology of Korea for its support.

[1] P. Verkerk, B. Lounis, C. Salomon, C. Cohen-Tannoudji, J.-Y. Courtois, and G. Grynberg, Phys. Rev. Lett. **68**, 3861 (1992).
[2] A. Hemmerich and T. W. Hänsch, Phys. Rev. Lett. **70**, 410 (1993).
[3] P. S. Jessen, C. Gerz, P. D. Lett, W. D. Phillips, S. L. Rolston, R. J. C. Spreeuw, and C. I. Westbrook, Phys. Rev. Lett. **69**, 49 (1992).
[4] M. Kozuma, Y. Imai, K. Nakagawa, and M. Ohtsu, Phys. Rev. A **52**, R3421 (1995).
[5] M. Kozuma, K. Nakagawa, W. Jhe, and M. Ohtsu, Phys. Rev. Lett. **76**, 2428 (1996).
[6] D. R. Meacher, D. Boiron, H. Metcalf, C. Salomon, and G. Grynberg, Phys. Rev. A **50**, R1992 (1994).
[7] W. D. Phillips and C. I. Westbrook, Phys. Rev. Lett. **78**, 2676 (1997); M. Kozuma, K. Nakagawa, W. Jhe, and M. Ohtsu, *ibid.* **78**, 2677 (1997).
[8] M. Weidemüller, A. Hemmerich, A. Görlitz, T. Esslinger, and T. W. Hänsch, Phys. Rev. Lett. **75**, 4583 (1995).
[9] G. Birkl, M. Gatzke, I. H. Deutsch, S. L. Rolston, and W. D. Phillips, Phys. Rev. Lett. **75**, 2823 (1995).
[10] A. Görlitz, M. Weidemüller, T. W. Hänsch, and A. Hemmerich, Phys. Rev. Lett. **78**, 2096 (1997).
[11] G. Raithel, G. Birkl, W. D. Phillips, and S. L. Rolston, Phys. Rev. Lett. **78**, 2928 (1997).
[12] P. Rudy, R. Ejnisman, and N. P. Bigelow, Phys. Rev. Lett. **78**, 4906 (1997).
[13] E. L. Raab, M. Prentiss, A. Cable, S. Chu, and D. E. Pritchard, Phys. Rev. Lett. **59**, 2631 (1987).
[14] J. Dalibard and C. Cohen-Tannoudji, J. Opt. Soc. Am. B **6**, 2023 (1989).
[15] M. Kasevich and S. Chu, Phys. Rev. Lett. **69**, 1741 (1992).
[16] A. Aspect, E. Arimondo, R. Kaiser, N. Vansteenkiste, and C. Cohen-Tannoudji, Phys. Rev. Lett. **61**, 826 (1988).